

Electronics Properties of Monoclinic HfO₂

Abdelkrim Mostefai^{1,*}, Smail Berrah², Hamza Abid¹

¹ Applied Materials Laboratory, University of Sidi Bel Abbes, 22000- Sidi Bel Abbes, Algeria

² LMER Laboratory, University of A/ Mira of Bejaia, Algeria

(Received 04 December 2017; revised manuscript received 04 December 2018; published online 18 December 2018)

Density functional theory (DFT) is a very successful technique to calculating the properties of many-electron systems from first principles. The bands structures, charge density and density of state (DOS) of monoclinic HfO₂ are calculated using Pseudo potential (PP) and Atomic Orbitals (AO) method, within the density functional theory DFT, generalized gradient approximation GGA and local density approximation LDA. Hafnium oxide (HfO₂) is a high-*k* dielectric (dielectric constant $k \sim 25$ at 300 K, band gap $E_g \approx 6$ eV); thermally stable up to 700 °C. HfO₂ is used in semiconductor manufacturing processes where they are usually used to replace a silicon dioxide gate dielectric.

Keywords: SiO₂, HfO₂, DFT, Aproximation LDA, Approximation GGA, ADF-BAND, Pseudo-potential (PP), Atomic orbitals (AO), Slater type orbitals (STO).

DOI: 10.21272/jnep.10(6).06026

PACS numbers: 71.15.Ap, 71.15.Mb

1. INTRODUCTION

Complementary metal oxide semiconductor (CMOS) devices have been going through an unprecedented progress during last three decades. The miniaturization of Metal-Oxide-Semiconductor field effect transistors (MOSFET) is insufficient to satisfy the performance specifications of International Technology Roadmap for Semiconductors (ITRS), different scaling limits for MOSFETs have been treated [1]. In this context, the gate oxide thicknesses reach limitations that make them permeable to leakage currents. Among various high-*k* dielectric materials, HfO₂ [2-6] (band gap $E_g \approx 6$ eV, dielectric constant $k \approx 25$ at 300 K, which is equal six times higher than that of SiO₂ ≈ 3.9) recently attracts much attention in the gate stack of MOSFETs due to their good thermal stability, it is considered to be the most attractive materials among the high dielectric materials.

HfO₂ is the most promising candidate to replace silicon dioxide SiO₂ [7, 8] in advanced metal oxide semiconductor devices (MOS) in gate stack and dynamic access memory devices.

HfO₂ exists in three crystal phases [9-11] (Figure 1). Low temperature monoclinic (space group P21/c). Medium temperature (Above 2000 °C) tetragonal (space group P42/nmc). High temperature (starting from 2700 °C) cubic (space group Fm3m).

2. COMPUTATIONAL METHOD

Calculations are based on density functional theory DFT and Slater Type Orbitals (STO) as basis functions. The generalized gradient approximation GGA (PBE) and local density approximation LDA are applied for the exchange-correlation potential, as implemented in the ADF-BAND code. Core electrons were treated by pseudopotentials; the potential of core states was treated in the frozen core approximation. The total number of basis functions for unit cell was 156. The monoclinic

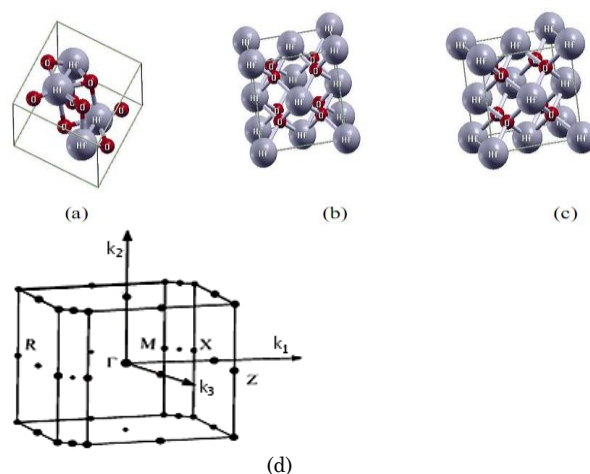


Fig. 1 – Crystal structure of HfO₂: (a) monoclinic phase, (b) tetragonal phase, (c) cubic phase, (d) Brillouin zones of monoclinic phases HfO₂. (The coordinates of the high-symmetry points in Brillouin zone are $\Gamma(0, 0, 0)$, $X(0.57, 0, -0.43)$, $Z(0.43, 0, 0.43)$, $M(0.43, 0, -0.57)$, $R(-0.43, 0, -0.43)$).

Table 1 – Calculated and experimentally determined structural parameters for monoclinic HfO₂. The Lattice parameters a , b , c and β . The internal parameters x , y , and z .

Atom	LDA	GGA	Exp. [14]
Lattice parameters	–	–	$a = 5.117$ $b = 5.175$ $c = 5.291$ $\beta = 99.22^\circ$
$x(\text{Hf})$	0.277	0.276	0.276
$y(\text{Hf})$	0.041	0.042	0.040
$z(\text{Hf})$	0.208	0.208	0.208
$x(\text{O1})$	0.070	0.069	0.074
$y(\text{O1})$	0.334	0.330	0.332
$z(\text{O1})$	0.343	0.345	0.347
$x(\text{O2})$	0.449	0.4445	0.449
$y(\text{O2})$	0.758	0.758	0.758
$z(\text{O2})$	0.479	0.478	0.480

* mostakrimo@yahoo.fr

HfO₂ is described by the lattice parameters, the internal parameters and space group P21/c. It is an electrical insulator with a band gap of 5 eV [12] to 5.8 eV [13].

3. RESULTS AND DISCUSSION

From the Figures 2, by comparing the structures bands calculated with both methods (LDA and GGA), we can note a difference in the value of the band gap width between the valence and conduction bands.

The top of the valence band is located at Γ , and the bottom of the conduction band in X (indirect gap).

We can say that the valence bands have less dispersion than the conduction bands. This is due to the fact that the electrons in the conduction bands are more free and therefore less localized.

Figure 3 shows the total DOS, Figures 4 shows the site-projected partial DOS O1, Figures 5 shows the site-projected partial DOS O2, and Figures 6 and 7 shows the site-projected partial DOS (Hf, Hf-d) for LDA and GGA approximation for monoclinic HfO₂. The bands from -17.3635 to -14.9063 eV (LDA) and -17.7197 to -15.2624 eV (GGA) are mainly due to O 2s orbitals (Brillouin Zone). The bands between -5.35045 -0 eV (LDA) and -5.29706 -0 eV (GGA) are mainly due to O 2p orbitals and Hf 5d orbitals (valence bands). The bands higher than 3.65 eV (LDA) and 3.71 eV (GGA) are mainly due to Hf 5d orbitals (conduction bands). The band gap of monoclinic phase (*m*-HfO₂) is 3.65 and 3.71 eV for LDA and GGA approximation, respectively. The results in this work, in good agreement with previous results [11, 15-18], Fiorentini and Gulleri performed theoretical calculations with GGA for a band gap of 5.7 eV [19].

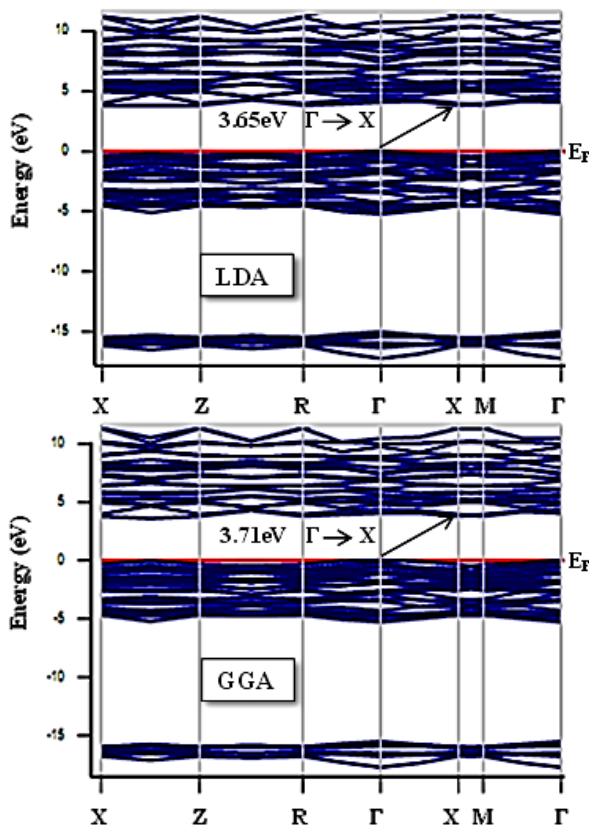


Fig. 2 –Band structure obtained by LDA and GGA

Another useful quantity for the analysis of the electronic properties, it is the electronic charge density of valence; this quantity is calculated by eliminating the core states. Figure 8 shows the contours of the charge density, charge are concentrated around the atomic spheres, whereas it is absent in the interstitial regions. This variation is a characteristic of metallic bonds.

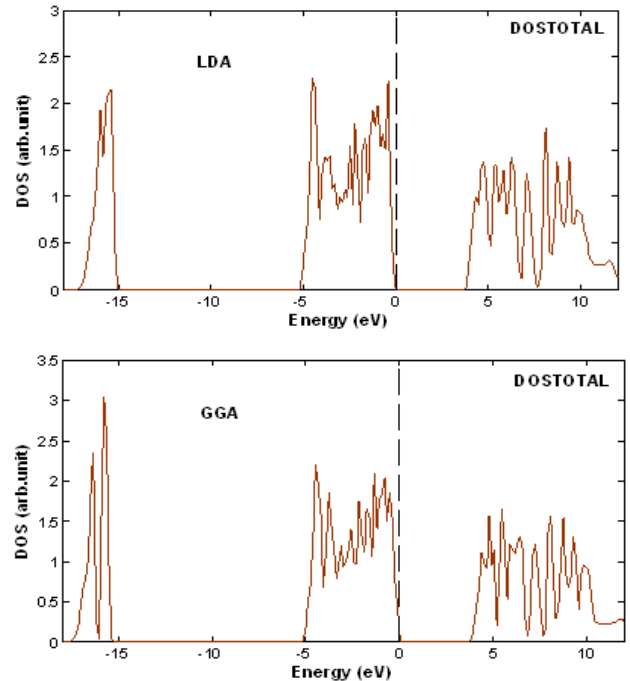


Fig. 3 –Total density of states (DOS) obtained by LDA and GGA

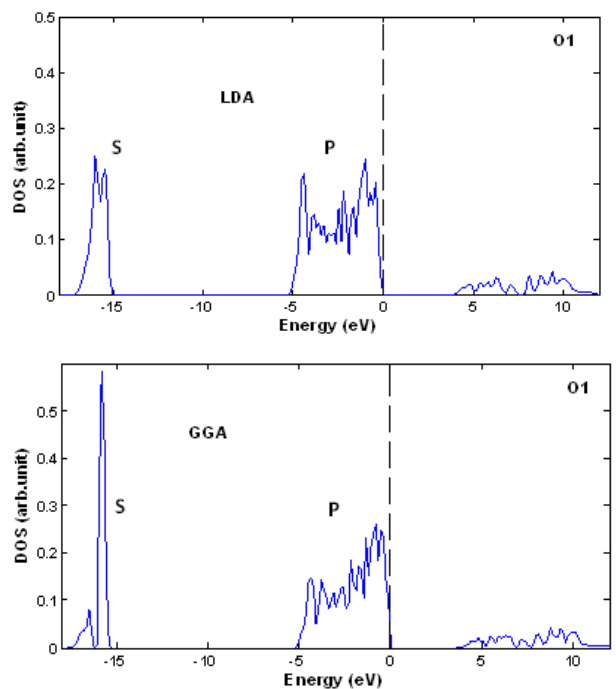


Fig. 4 –Partial density of states (DOS) O1 obtained by LDA and GGA.

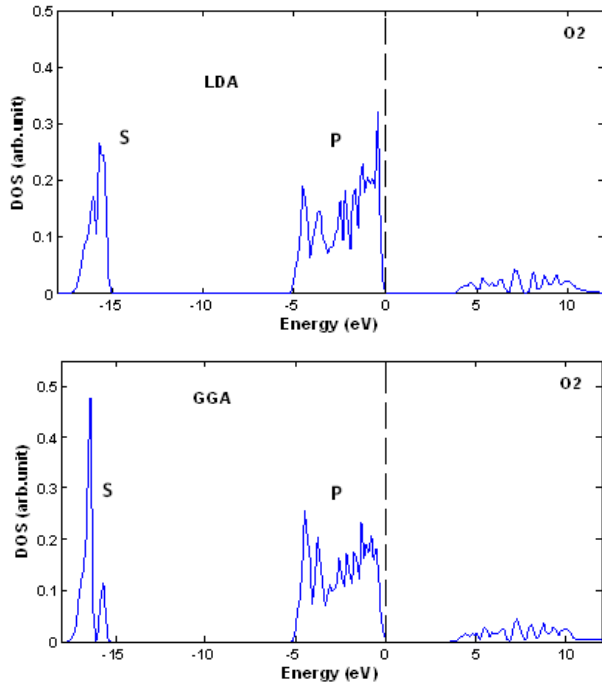


Fig. 5 –Partial density of states (DOS) O2 obtained by LDA and GGA

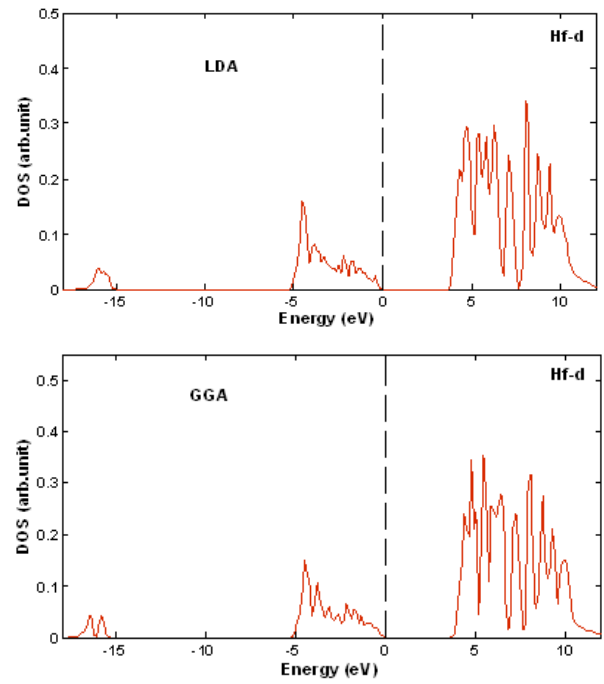


Fig. 7 –Partial density of states (DOS) Hf-d obtained by LDA and GGA.

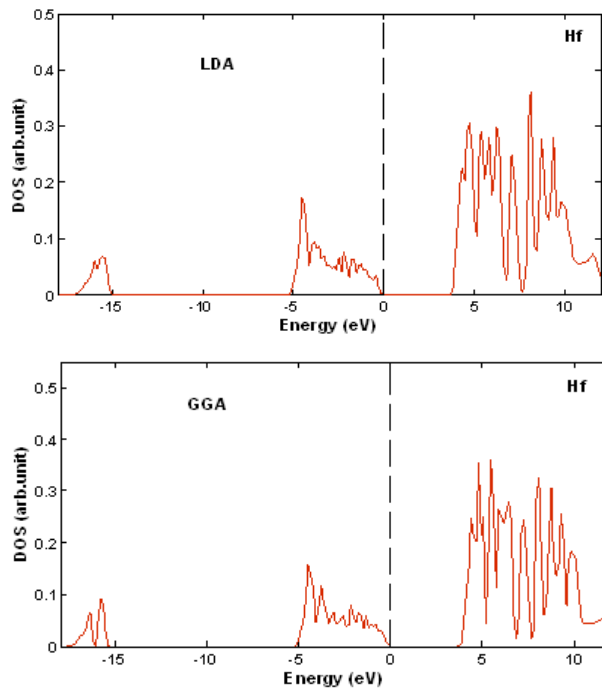


Fig. 6 –Partial density of states (DOS) Hf obtained by LDA and GGA

Bands structures, density of states and charge density of monoclinic HfO₂ have been investigated using the slater type orbital STO and pseudo-potential approach based on the first-principles density functional theory (DFT) within the generalized gradient approximation (GGA (PBE)) and local density approximation LDA.

The analysis of the density of states (DOS) allows knowing the distribution and occupation of electronic states of the oxide compared to the Fermi level.

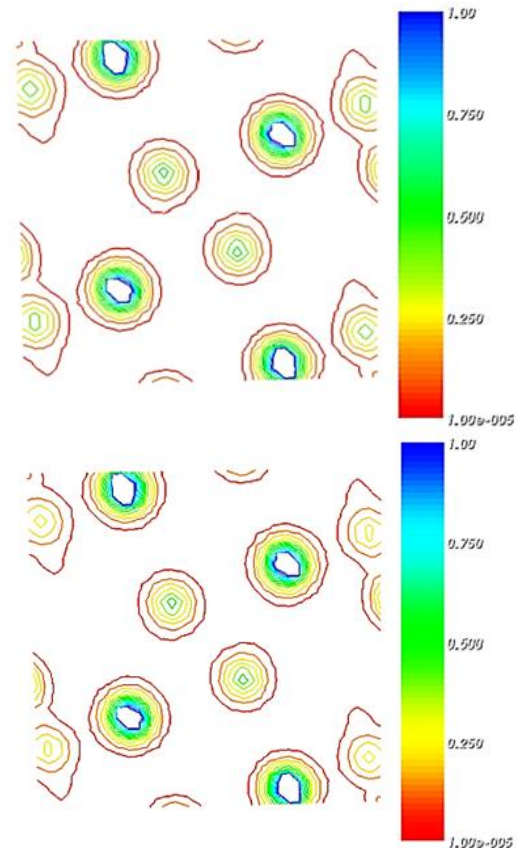


Fig. 8 – Contours of charge density (in $e/\text{\AA}^3$) obtained by LDA and GGA.

The analysis of the partial density of states of HfO₂ makes it possible to know the electronic states contributing to the different sub-bands of the total density of states.

4. CONCLUSION

Bands structures, density of states and charge density of monoclinic HfO₂ have been calculated. m-HfO₂ has a smaller dielectric constant by contribution to the tetragonal and cubic phase. Electronic properties for the monoclinic HfO₂ have been performed with first-principles density functional theory (DFT) and Atomic

Orbitals (AO) method. We used two approximations to determine the exchange-correlation potential, the generalized gradient approximation GGA (PBE) and local density approximation LDA. This will allow us to know the distribution and occupation of electronic states of the oxide compared to the Fermi level.

This study is important for determining the nature and formation of structural bonds.

REFERENCES

1. A. Mostefai, S. Berrah, H. Abid, *J. Elec. Eng.* **17** N 1, 74 (2017).
2. X.H. Zheng, A.P. Huang, Z.C. Yang, Z.S. Xiao, M. Wang, G.A. Cheng, *Acta Phys. Sin.* **60**, 017702 (2011).
3. S. Monaghan, P.K. Hurley, K. Cherkaoui, M.A. Negara, A. Schenk, *Solid State Electron.* **53**, 438 (2009).
4. K. Xiong, J. Robertson, *Microelectron. Eng.* **80**, 408 (2005).
5. S.Y. Zhu, J.P. Xu, L.S. Wang, Y. Huang, *Chinese Phys. B* **22**, 097301 (2013).
6. K. Xiong, J. Robertson, M.C. Gibson, S.J. Clark, *Appl. Phys. Lett.* **87**, 183505 (2005).
7. G.D. Wilk, R.M. Wallace, J.M. Anthony, *J. Appl. Phys.* **89**, N°10, 5243 (2001).
8. J. Robertson, *Eur. Phys. J. Appl. Phys.* **28**, 265 (2004).
9. R. Terki, G. Bertrand, H. Aourag, C. Coddet, *Mater. Lett.* **62**, 1484 (2008).
10. M.A. Caravaca, R.A. Casali, *J. Phys. Condens. Matter.* **17**, 5795 (2005).
11. T.V. Perevalov, V.A. Gritsenko, S.B. Erenburg, A.M. Badalyan, H. Wong, C.W. Kim, *J. Appl. Phys.* **101**, 053704 (2007).
12. S. Toyoda, J. Okabayashi, H. Kumigashira, M. Oshima, K. Ono, M. Niwa, K. Usuda, N. Hirashita, *J. Electron. Spectrosc. Relat. Phenom.* **137-140**, 141 (2004).
13. A. Callegari, E. Cartier, M. Gribelyuk, H.F. Okorn-Schmidt, T. Zabel, *J. Appl. Phys.* **90**, 6466 (2001).
14. X. Zhao, D. Vanderbilt, *Phys. Rev. B* **65**, 233106 (2002).
15. T.V. Perevalov, A.V. Shaposhnikov, K.A. Nasyrov, D.V. Gritsenko, V.A. Gritsenko, V.M. Tapilin, *Defects in High-Gate Dielectric Stacks: Nano-Electronic Semiconductor Devices*, 423 (Dordrecht: Springer: 2006).
16. A.A. Demkov, *phys. status solidi b* **226**, 57 (2001).
17. L. Qi-Jun, Z. Ning-Chao, L. Fu-Sheng, L. Zheng-Tang, *Chin. Phys. B* **23** N 4, 047101 (2014).
18. J. Li, J. Han, S. Meng, H. Lu, A. Tohyama, *Appl. Phys. Lett.* **103**, 071916 (2013).
19. V. Fiorentini, G. Gulleri, *Phys. Rev. Lett.* **89**, 266101 (2002).